ACOUSTIC WAVE SCATTERING FROM A CIRCULAR CRACK: COMPARISON OF DIFFERENT COMPUTATIONAL METHODS

William M. Visscher

Theoretical Division, MS B262
Los Alamos National Laboratory
Los Alamos, NM 87545

INTRODUCTION

This work was motivated by a disagreement between the results obtained from two computations of scattering of an axially incident elastic p-wave on a circular crack. One calculation, using the method of Mal [1], involving the direct solution of the Helmholtz integral equation for this case, shows the total cross-section oscillating with a considerable amplitude about $\sigma_{tot} = 2\pi a^2$ as a function of $k_R a$ with period π, where $k_R = 2\pi/\lambda_R$ is the Rayleigh surface wavenumber. Another calculation, [2] using MOOT, in which the elastic displacement near the crack is expanded in regular spherical eigenfunctions of the elastic wave equation, agrees with the first calculation reasonably well up to $k_R a = 10$ or so, but thereafter

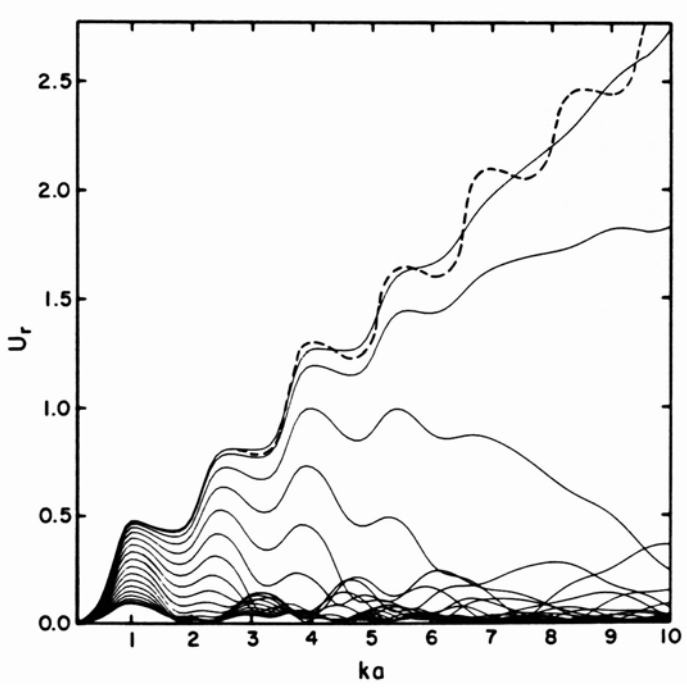

Fig. 1. Elastic wave scattering from a circular crack. The solid lines are the ρ-ρ backscattering amplitudes from a crack oriented broadside (top) to edge-on (bottom) in 5° intervals, computed using MOOT with spherical eigenfunctions of the elastic wave equation as basis functions. The dashed line is obtained from Mal's solution for the axisymmetric (broadside) case. The oscillations in the Mal solution (thought to be quite accurate) continue to large ka, while the oscillations in the MOOT results damp rapidly. From Opsal and Visscher [2].

the oscillations in σ_{tot} rapidly disappear. Figure 1 contrasts the different results.

We thought that perhaps the reason for this discrepancy was that the basis for the MOOT expansion ($j_n(kr)$ and its derivatives) was inappropriate; in fact, we mistakenly stated that it is not complete on $0 < kr < ka$ (it is complete; see 9.1.86 in ref. [3]), and that the difference might be ameliorated by a different choice of basis.

A simple system on which to test this speculation is the scalar wave incident on a circular crack. The wave function ϕ satisfies

$$(\nabla^2 + k^2)\phi = 0 \quad , \tag{1}$$

asymptotic scattering conditions, and certain boundary conditions (BC's) on the crack surface C. The crack is shown on Fig. 2; it is a mathematical crack (zero thickness) in the xy plane with radius a.

The simplest BCs to impose on ϕ would be Dirichlet ($\phi = 0$ on C) or Neumann ($\phi_{,n} = 0$ or C, where $\phi_{,n} = \hat{\nabla}\phi\cdot\hat{n}$). The scattering can be obtained for these cases by a variety of methods. The T-matrix of Waterman has been obtained for both Dirichlet and Neumann BCs [4]. The Helmholtz integral equation has been solved for Dirichlet BCs and axial incidence [5], and MOOT has been applied to this case, with two different choices for the basis set [5].

Unfortunately, though, all these methods give results (for the Dirichlet case; not all have been worked out for Neumann BCs) which agree with one another; in particular, for large ka no oscillations appear in the scattered amplitude. This is a reflection of the fact that for large ka and Dirichlet BCs $\phi_{,n}$ on C approaches a constant (independent of $\rho = \sqrt{x^2+y^2}$) [5].

In contrast, the elastic wave case illustrated in Fig. 1 has oscillations in the scattered amplitude caused by resonance modes (drumhead vibrations) which are standing surface waves on the crack surface (this is why the oscillations in Fig. 1 have roughly period π in $k_R a$).

The reason for this difference is that the Helmholtz equation (1) admits no surface wave solutions with either Dirichlet or Neumann BCs, and without surface waves one can't get standing waves on C and one won't get resonance oscillations in the scattered amplitude. Our model is just too simple to exhibit the effect we wish to study.

A solution to this problem is to change the BCs to mixed boundary conditions (MBCs)

$$\phi + \gamma\phi_{,n} = 0 \quad \text{on C} \quad , \tag{2}$$

which admits, with (1), a solution

$$\phi(x,y,z) = e^{i\vec{\kappa}\cdot\vec{\rho}-\gamma z} \tag{3}$$

with $\kappa^2 = k^2 + \gamma^2$. Equation (3) describes a surface wave if the surface is $z = 0$, $\gamma > 0$, and the incompressible fluid occupies the upper half-space. If we solve the crack problem with the BCs (2), one expects to see resonances corresponding to standing surface waves on the crack surface.

The MBCs however, complicate the mechanics of solving the scattering problem considerably. The T-matrix method can no longer be applied, because a feature of the method which is essential to its application to cracks, the symmetry of the Q-matrix, no longer holds (or at least has not been demonstrated).

The Helmholtz integral equation method, too, becomes much more difficult. The Helmholtz integral equation is

$$\phi(r) = \phi_0(r) - \int_C \{G(r,r')\phi_{,n'}(r') - G(r,r')_{,n'}\phi(r')\}dS' \quad , \qquad (4)$$

for r outside the crack C, with $G(r,r') = e^{ikR}/4\pi R$, $R = |\vec{r}-\vec{r}'|$. For axial incidence, $\phi_0(r) = e^{ikz}$, and in order to solve (4) for $\phi(r)$, r on S, one considers $\phi_+(r)$, and $\phi_-(r)$, which are $\phi(\rho,+0)$ and $\phi(\rho,-0)$ respectively. It can be shown that

$$G(r,r')_{,z} = -\frac{\mathrm{sgn}(z-z')}{4\pi\rho}\,\delta(\rho-\rho')$$

for z, z' small, so that (4), with (2), yields

$$\bar{\phi}(\rho) = 1 + \gamma^{-1}\int_{C+} G(\rho,\rho')\bar{\phi}(\rho')dS' \quad , \qquad (5)$$

with $\bar{\phi} = \frac{1}{2}(\phi_+ + \phi_-)$ and C+ = top surface of crack. Equation (5) can be solved for $\bar{\phi}(\ell)$, which, when inserted in (4), will give the even (in z) part of $\phi(r)$.

In order to obtain an equation for $\hat{\phi} = \frac{1}{2}(\phi_+ - \phi_-)$, which, when plugged into (4) will give the odd part of $\phi(r)$, one needs to differentiate (4) with respect to z before letting $z \to \pm 0$. This yields

$$-\gamma^{-1}\hat{\phi}(\rho) = ik - \int_{C+} G_{,zz}(\rho,\rho')\hat{\phi}(\rho')dS' \quad , \qquad (6)$$

with

$$G_{,zz} = \left.\frac{d^2G}{dz^2}\right|_{z=z'=0} \quad . \qquad (7)$$

Equation (6) is a much nastier one than (5), because (1) has a $|\vec{\rho}-\vec{\rho}'|^{-3}$ singularity. Although it turns out that this is no problem in principle (the singularity is integrable, and one can replace the surface integral with a "principal value" integral by omitting a small circle around $\rho' = \rho$), it is a serious one in practice because it drastically worsens the convergence of the Fourier integrals with which it is natural to represent (7).

This leaves us only MOOT with which to compute acoustic scattering from a crack with MBCs.

Moot

We will now briefly sketch the method of optimal truncation (MOOT), as applied to circular flat cracks. It will be clear that it is applicable to calculation of a scattering from any isolated flaw.

The idea is to expand ϕ in truncated sets of eigenfunctions of the Helmholtz operator (1) independently in each of the regions I, II, and III shown on Fig. 2. Then integrate the square of the residual (the amount by which the BCs or matching conditions fail) on the surfaces $S_\pm$ and C_I. Thus

$$I = \int_C \{|\phi_I + \gamma\phi_{I,n}|^2 + |\phi_{II} + \gamma\phi_{II,n}|^2\}dS$$

$$+ \int_{S+} \{|\phi_0 + \phi_{III} - \phi_I|^2 + \beta/k^2\ |\phi_{0,n} + \phi_{III,n} - \phi_{I,n}|^2\}dS$$

$$+ \int_{S-} \{|\phi_0 + \phi_{III} - \phi_{II}|^2 + \beta/k^2\ |\phi_{0,n} + \phi_{III,n} - \phi_{II,n}|^2\}dS \quad , \tag{8}$$

where $\phi_I(r) = \sum_{n=1}^{N} a_n\phi_n(r)$, $\phi_{II}(r) = \sum_{n=1}^{M} b_n\phi_n(r)$,

and $\phi_{III}(r) = \sum_{\ell=0}^{\ell_{max}} c_\ell h_\ell^{(1)}(r)Y_\ell^0(\cos\theta)$, $\phi_0(r) = e^{ikz}$

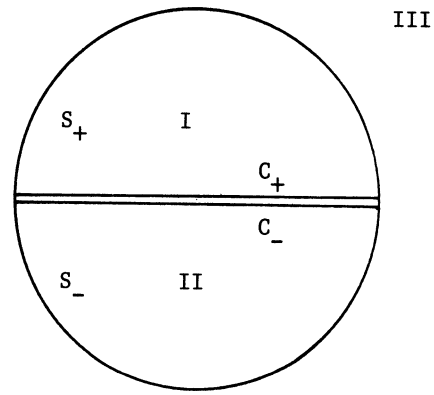

Fig. 2. The circular crack on the xy plane. $S_\pm$ are the upper and lower hemispheres surrounding C_+, the top and bottom surfaces of the circular crack.

β is a dimensionless constant we take to be $\min(1,(ka)^{-2})$. Varying it by an order of magnitude either way has little effect on results. Clearly $I \geq 0$, with equality attained if and only if ϕ_I, ϕ_{II}, ϕ_{III} comprise an exact solution of the scattering problem with ϕ_0 incident. The functions $\phi_n(r)$ are any convenient set of solutions of $(\nabla^2+k^2)\phi_n = 0$; they need not be mutually orthogonal. The truncation limits N, M, ℓ_{max} are mostly dictated by the value of ka we consider. Although there is in principle no reason they can't be different, we will take $N = M = \ell_{max} + 1$.

Now I is a bilinear form in $\alpha_n = \{a_n, b_n, c_n\}$, which we wish to minimize. Thus

$$\frac{\partial I}{\partial \alpha_n^*} = 0$$

is a set of 3N linear inhomogeneous equations for the 3N unknowns a, b, c, with coefficients which are integrals of pairwise products of ϕ_0, ϕ_n, and

$Y_\ell^0(\cos\theta)$ on C_+ and S_+. The matrix of the coefficients can be readily inverted (at least if N is not too large), and the solution for α_n obtained.

So MOOT is uniquely specified except for choosing ϕ_n, the set of N independent solutions of (1) with which ϕ in the upper and lower hemisphere is represented. We will choose two sets, and compare the results. The first choice will be

$$\phi_n = j_n(kr)\, Y_n^0(\cos\theta) \quad , \tag{9}$$

in analogy with the set used in [2] to compute elastic wave scattering from the circular crack. The second choice will be

$$\chi_n = J_0(p_n\rho) \begin{matrix} \sin q_n z \\ \cos q_n z \end{matrix} \quad , \tag{10}$$

where p_na are the roots of $J_0(x)$ and of $J_0'(x)$, and $p_n^2 + q_n^2 = k^2$. Most of the q_n's are imaginary. Both (9) and (10) comprise complete sets as $N \to \infty$; the question we wish to address here is "which set will closely approximate the correct answer with the least labor?"

Numerical Considerations

In the case of Dirichlet BCs the solution for $k \to 0$ is for r on C

$$\phi_{,n}(\rho) = -2/\pi\sqrt{a^2-\rho^2} \quad , \tag{11}$$

and this inverse square root singularity at the crack edge is presumably preserved for all k. For the mixed BCs (2) the behavior of $\phi_{,n}$ and consequently also of ϕ is undoubtedly also singular at $\rho = a$, but we don't know the nature of the singularity. If $\phi_{,n}$ for MBC (and consequently also ϕ) behaves like (11), then the integrals on C in I will contain logarithmic divergent terms, presumably cancelling one another. Since we don't know the nature of the singularity, however, we will proceed as if there were none, and let the results tell us what it is.

Most of the integrals which are the coefficients of the bilinear form (8) must be performed numerically, which we do by Gauss-Legendre quadrature with 50 points (on the interval $0 < \rho < a$ for the C-integrals; on the interval $0 < \cos\theta < 1$ for the S-integrals).

We will show results of calculations for a variety of choices of ℓ_{max}, up to 24, and for values of ka up to 14. For these values of ℓ_{max} 50 in the Gauss-Legendre quadrature is more than adequate; whether $\ell_{max} = 24$ is sufficient for ka = 14 can be judged from the results.

RESULTS

In Fig. 3 is shown the value of $Re\phi$ on the top surface of the crack as a function of ρ and ℓ_{max} computed with MOOT using a spherical basis. The phase of ϕ has been adjusted here so that it is real in each case at $\rho = 0$. This is for ka = 10; ϕ does not approach its true value until $\ell_{max} \geq 15$. Even for ka = 0 ϕ has 3 nodes in $0 < \rho < 1$, and one always needs $\ell_{max} \geq 15$ or so for accurate results.

Figure 4 shows I/I_0 and 4π Im $f(0)/k\sigma_{TOT}$ (the optical theorem ratio) for this system. $I/I_0 = 0$ for an exact solution. It doesn't vanish, but seems to be decreasing as ℓ_{max} increases as if the MOOT solution is trying,

with slow success, to accommodate a singularity (Fig. 3 shows a discontinuity) in ϕ at $\rho = 1$. The optical theorem ratio should be unity; it is about 0.98 and increasing at the largest ℓ_{max}.

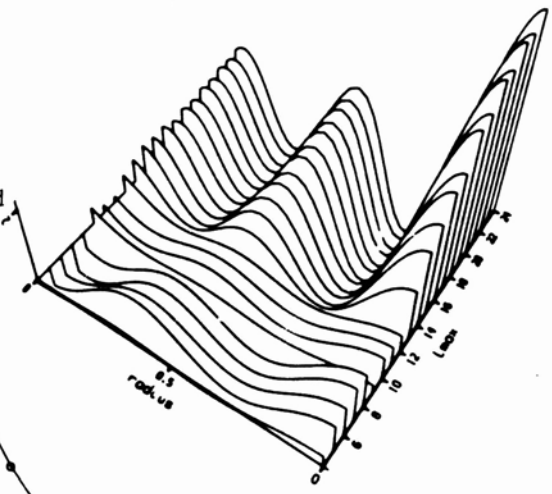

Fig. 3. Pressure Reϕ on the top surface of a circular crack of unit radius caused by an axially incident wave with ka = 10. As ℓ_{max} increases, ϕ seems to converge nicely, except at $\rho = 0$. But the importance of $\phi(0)$ is diminished by the fact that $\phi(\rho)$ is always weighted with $\rho d\rho$. $\phi(\ell)$ begins to resemble its true value at $\ell_{max} \sim 15$. This figure was computed using spherical basis functions.

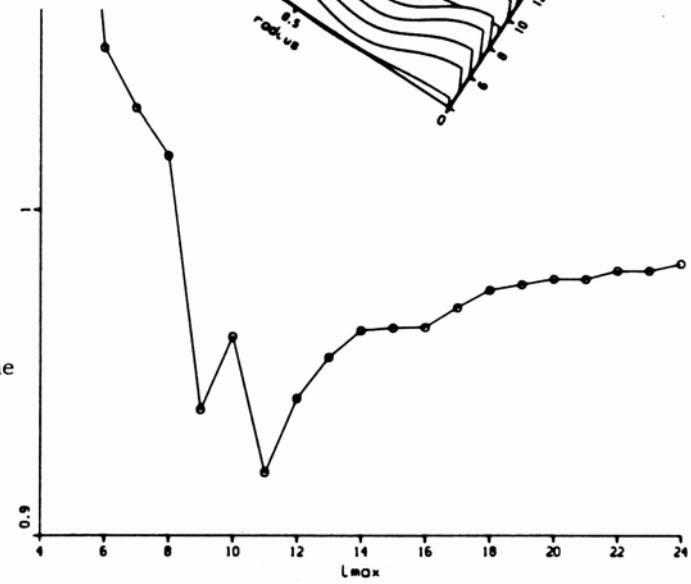

Fig. 4. Integrated residual I/I_0 (left ordinate scale) and optical ratio (right ordinate scale) for the system described in Fig. 3. I_0 is I with only $\phi_0 \neq 0$.

The next two figures illustrate the same quantities for the cylindrical basis set. The results are similar.

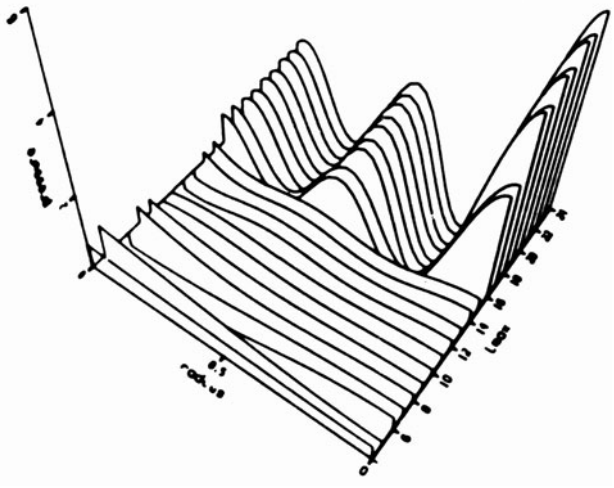

Fig. 5. Same as Fig. 3, but using cylindrical basis functions. This ϕ agrees with that of Fig. 3 for large ℓ_{max}. The relatively more sudden change from noise to nearly the correct ϕ at $\ell_{max} \sim 15$ is caused by the fact that at that point the number of nodes and antinodes in $J_0(p_n\rho)$ in $0 \leq \rho \leq 1$ coincides with the number in the correct $\phi(\rho)$.

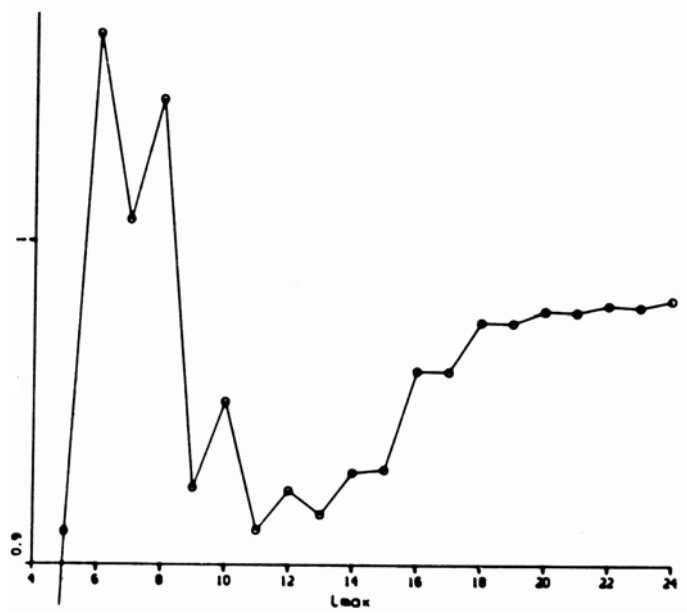

Fig. 6. Same as Fig. 4, but for cylindrical basis functions.

The final series of figures shows how some of the same quantities vary as ka goes from 0.5 to 14 for the circular crack with spherical basis functions ($\ell_{max} = 24$) and with cylindrical basis functions ($\ell_{max} = 23$). The residual integral plots indicate the trustworthiness of the calculation. Figures (7) and (9) are in close agreement (notice the different vertical scales).

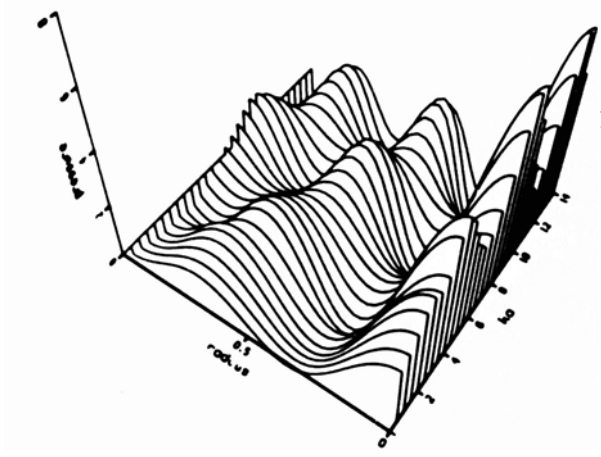

Fig. 7. Real part of ϕ calculated by MOOT with spherical eigenfunctions and $\ell_{max} = 24$ as a function of ρ and ka. Standing waves exist on this crack even for ka = 0; the number of nodes increases more or less linearly with ka.

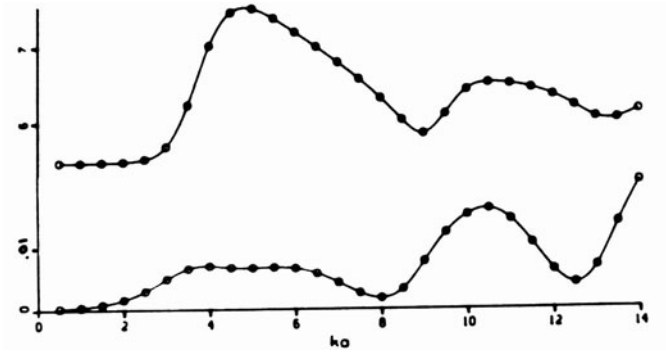

Fig. 8. Residual integral and total cross-section for the system described in Fig. 7. The cross-section approaches a constant for ka → 0; for large ka it seems to oscillate about $2\pi a^2$, the short-wavelength limit.

CONCLUSIONS

Our results indicate that our original speculation, that the discrepancy of Fig. 1 was caused by inadequacy of the spherical basis set, was wrong. In application to the present test problem, in fact, the spherical basis set works better than the cylindrical one does. Both are quite capable, with the same truncation limit $\ell_{max} = 24$, of accurately describing the pressure (analog of the crack-opening-displacement in the elastic wave scattering case) at least up to ka = 14, when the pressure has 5 nodes in $0 < \rho < a$.

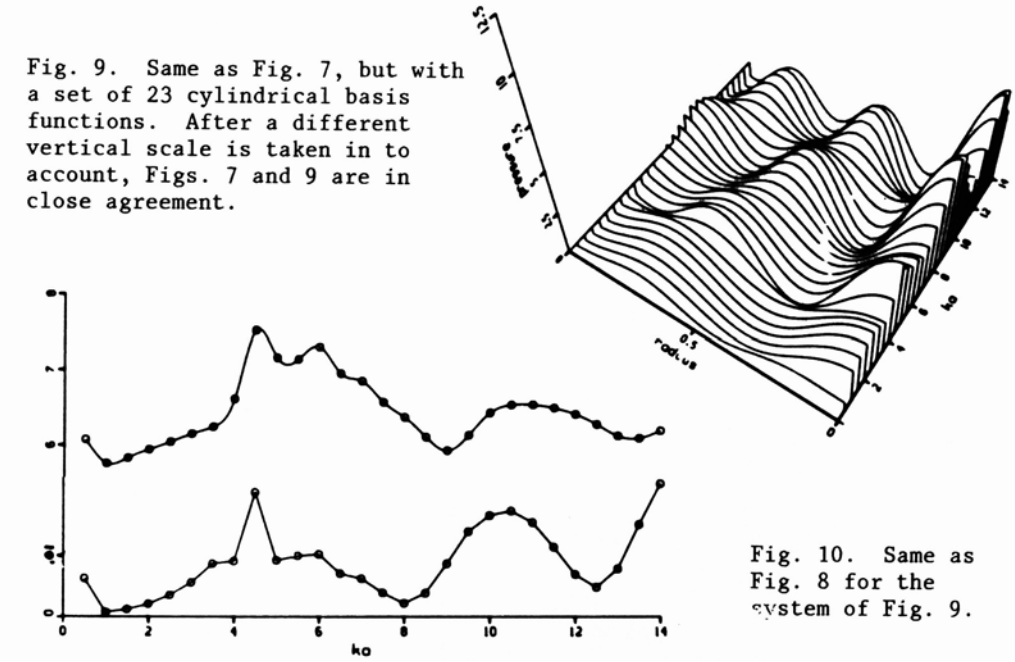

Fig. 9. Same as Fig. 7, but with a set of 23 cylindrical basis functions. After a different vertical scale is taken in to account, Figs. 7 and 9 are in close agreement.

Fig. 10. Same as Fig. 8 for the system of Fig. 9.

The original question then returns: if it is not due to a bad basis set, what does cause the difference between the two results on Fig. 1? Discounting the possibility that Mal's method yielded wrong results here, one is forced to the conclusion that ℓ_{max} was not large enough in the MOOT calculation reported in [2]. A rough estimate, obtained from the results of the present scalar MBC problem, of the minimum ℓ_{max} required for a given ka $\gg$ 1, is

$$\ell_{max} \gtrsim 1.5ka \quad . \tag{17}$$

The largest value of $k_R a$ shown in Fig. 1 is $k_R a = 21.4$ ($k_\rho a = 10$); the criterion (17) indicates that in order to insure accuracy to this value of ka one should take $\ell_{max} \gtrsim 30$. The ℓ_{max} used in the MOOT calculation of [2] was only 20. It may be repeated with larger ℓ_{max} to see if this conjecture is correct.

REFERENCES

1. A. K. Mal, Int. J. Eng. Sci. 8, 381 (1970).
2. Jon L. Opsal and William M. Visscher, J. Appl. Phys. 58, 1102 (1985).
3. M. Abramowitz and I. A. Stegun, "Handbook of Mathematical Functions," (National Bureau of Standards, 1964).
4. Gerhard Kristensson and P. C. Waterman, J. Acoust. Soc. Am. 72, 1612 (1982).
5. William M. Visscher, unpublished.